

Fiber to resonator coupling multicriteria optimization with COMSOL multiphysics

Patrice Salzenstein¹, David Bassir^{2,3}, David Perez de Lara^{4,5}

¹Centre National de la Recherche Scientifique (CNRS), UBFC, FEMTO-ST Institute, Besançon, FRANCE
patrice.salzenstein@femto-st.fr

² CNRS, CMLA – ENS Cachan, Université Paris Saclay, FRANCE

³IRAMAT, UMR –7065, Université Technologique de Belfort-Montbéliard (UTBM), Université de Bourgogne Franche-Comté (UBFC), Belfort, FRANCE
david.bassir@cmla.ens-cachan.fr

⁴Materials Science and Engineering Department, Guangdong Technion Israel Institute of Technology, Shantou, CHINA

⁵Zhejiang Beyond sun Green Energy Technology Co., Ltd. Zhejiang, CHINA
david.perezdelara@gtiit.edu.cn

ABSTRACT

In this paper, we discuss the principle of coupling an optical signal to an optical resonator. We give the broad outlines of the principle and the experimental parameters then we look at how to optimize this coupling using finite element simulations on COMSOL software. Simulation of the coupling is based on straight and ring waveguides placed very close to each other so the waveguide can be transmitted from one to other.

KEYWORDS

Optical resonator, Coupling, optimization, COMSOL wave guide

1. INTRODUCTION

We have seen that optical resonators with a very high quality factor, at least 100 millions, are useful for various types of applications in metrology, sensors or oscillators [1 – 5]. Studies in the literature concerning the modeling of coupled device based on optical fiber with crystalline resonators which involve the aspect of simulation and optimization [1 – 7]. It is also necessary to take into account the technological constraints of manufacture for the coupling [8]. The first step of multi-criteria optimization shows that we can simulate and then find an optimal design. The sensitivity analysis shows a relatively good correlation between the experimental Q factor obtained, and that obtained with the simulation by the finite elements. This optimization process incorporates certain constraints related to the manufacturing process, and to the thermal analysis of the resonator. However, some parameters require a domain which is non-continuous, it is chosen between fixed positions, but this makes the convergence more complicated to achieve. We therefore focus on the implementation of the experimental concept and on the coupling of crystalline resonators under a straight waveguide and the simulation is based on the multi-physics software COMSOL [9 – 11]. We present simulation results and also the comparison with the experiment.

2. COUPLING OF A RESONATOR TO A GUIDE

2.1. Need to couple the optical resonator

If we want to mount optical resonators in oscillator mode, or if it is simply necessary to characterize it, it is

necessary to proceed by coupling. An optical resonator considered as a cavity could be ideal if we had a totally closed system being isolated from the world outside. The propagation of a signal inside this cavity could then correspond to a high and intrinsic quality coefficient of the resonator. Nevertheless, in reality, an optical resonator, i. e. a resonant cavity, is not a closed system at all. We must measure its quality coefficient parameters. However, it is obvious that any external intervention could break the insulation of a cavity. It is necessary to be able to inject and of course recover the information. The main objective is to inject an optical signal inside the cavity. Figure 1 shows how a resonator is coupled to an optical tapered fiber. There are of course other methods to inject a signal. What comes to mind first is to illuminate the cavity with lighting of which the power would be quite significant. However, this method could not highlight the strong quality coefficients, which, at the opposite, require a certain finesse. There is the possibility of sending a signal by using a prism, which is convenient in the case of a compact and robust component. We could also use a tapered fiber or tip, which approaches the resonator sufficiently closer to be able inject signal in the resonant cavity. The method we find easier to do in the lab is to use a stretched and tapered fiber. We first remove the sheath of the fiber, then we stretch from each end, performing this stretch under a flame [12]. We therefore act on the principle that the resonator is coupled to a tapered fiber.

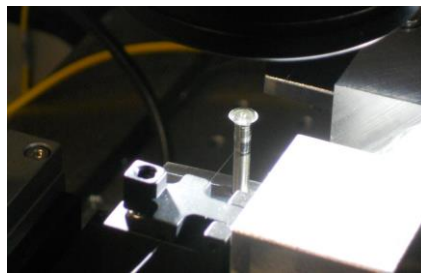


Fig. 1: Photograph of an optical resonator coupled to a tapered optical fiber.

2.1. Main active parameters

References	e	L	g	D	Q-factor
Colombia University & University of California, Si ₃ N ₄ [14]	750nm	N-C	N-C	N-C	6.6x 10 ⁶
Cornell University, Si ₃ N ₄ [15]	644nm	900nm	N-C	20μm	3x 10 ⁶
Cornell University, Si ₃ N ₄ [13]	910 nm	1.8 μm	680nm	115μm	7x 10 ⁶
Femto-st Institute, Si ₃ N ₄ [17]	1μm	3μm	600nm	90μm	1x 10 ⁵
Guangxi University, Silicon [16]	320nm	500nm	160nm	40μm	N-C

Table 1: Table of the main parameters for silicon nitride microrings and their coupling to a ridge realized on a chip. (*e*, *L*) refer respectively to the thickness and to the width of the Si₃N₄ microring and the ridge. (*D*, *g*) refer respectively to the diameter and to the gap between the Si₃N₄ microring and the ridge. N-C (Not Known) show that the parameter was not described or listed in the reference.

In Table 1, we give the typical parameters that are involved in the comparison of the Q factor for optical resonators of micro disk type. They are all silicon nitride on a silicon chip so they are better comparable. Unfortunately, not all references describe and give full details of their experiences. However, it is very interesting to give a narrow range of variation of the factor Q obtained as well as the associated parameters such as the thickness, the diameter and the width of the micro ring Si₃N₄ and of the ridge. Authors at Cornell University have obtained a good Q-factor with a propagation loss within the ring equal to 4.2 dB/m and we estimate the absorption loss to be 71%.

2. 3. Main parameters for the crystalline material: MgF₂ and Ca F₂:

For analysis, we select two materials. The first material is the Magnesium Fluoride (MgF₂), which is characterized by its refractive index, for the ordinary and extraordinary ray between (No, Ne) respectively equal to 1.37 and 1.38, for a Transmission Range between 0.12 and 8.5 μm. The MgF₂ is density is 3.148g/cm³. The second material is the Calcium fluoride (CaF₂), which is characterized by its refractive index for the ordinary and extraordinary ray between (No, Ne) respectively equal to 1.42 and 1.44 with a Transmission Range between 0.2 and 9 μm. The CaF₂ is density is 3.18g/cm³. Typical parameters are involved in the Q-factor comparison for the silicon nitride micro-rings and ridge on a silicon chip. We have reported the results in reference [18]. A number of references give a more accurate picture of typical parameters [13 – 16]. Thickness is between 320 nm and 910 nm. Width of the Si₃N₄ micro-ring vary in the range of 500 nm to 1.8 μm, when diameter of the ring vary from 20 to 115 μm. Gap between the Si₃N₄ micro-ring and the ridge is in between 160 and 680 nm. Figure 1 gives a better understanding of the various parameters mentioned for coupling to a micro-ring. Q-factors are up to 7x 10⁶. Cornell University have obtained a good Q-factor with a propagation loss within the ring equal to 4.2 dB/m and we estimate the absorption loss to be 71%. These performances are interesting. However, it is clear that the micro-rings quality factors are not as high as are those obtained with crystalline resonators. We concretely have selected two different materials for the sensitivity analysis. The first one is Magnesium Fluoride (MgF₂). It is characterized by its refractive index. For the ordinary and extraordinary ray between (No, Ne), it is respectively equal to 1.37 and 1.38 with a transmission in the range 0.12 – 8.5 μm. Density of MgF₂ is 3.148g/cm³. The second chosen material is Calcium fluoride (CaF₂). Its refractive index for the ordinary and extraordinary ray between (No, Ne) is respectively equal to 1.42 and 1.44. Its transmission is in the range 0.2 – 9 μm. Its density is 3.18g/cm³.

3. MODELLING OF THE COUPLED DEVICES

We look at the coupling between a thin fiber and a resonator. One can refer for the coupling of resonators to a paper, which concerns another type of resonator, the micro-spheres [7]. We can make some analogies between the propagation of an optical signal and that of a microprobe signal along a coplanar line [19]. The design problem that has been studied in order to maximize the factor (Q) is described in the figure 2.

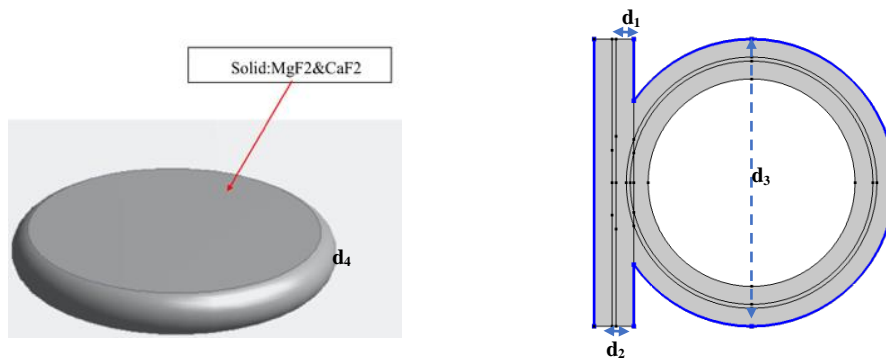


Fig. 2: 3D & 2D views of the design parameters used for the optimization process. The contour represent the boundary condition as we need to model the gap in the air.

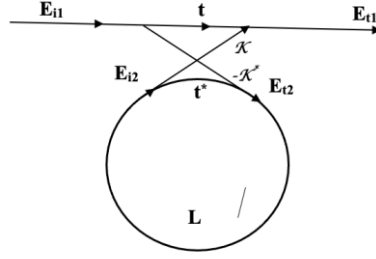


Fig. 3: Relation between the incident and the transmitted/coupled fields in term of coupling coefficients and, as well as the round-trip loss.

The value d_1 refer to the gap between the fiber and resonator (which should be less than the λ in the center of the fiber), d_2 is the optical fiber diameter, d_3 is the inner diameter of the resonator, and d_4 is the external diameter. Modelling is based on the following references [20 – 24]. Because of the optical symmetry and the Gallery mode in the resonator, we assume that the main phenomena will take place at the close circumferential structure of the resonator disc. For the Final element modelling, we reduce the study at the circumference area of the resonator. In the following simulation, we have included the discontinuity at the boundary between the straight waveguide and the ring waveguide. This integration of the phase discontinuity and thereby the discontinuity in the field envelope, \mathbf{E}_1 , a Field Continuity boundary condition is used at the boundary between the straight waveguide and the ring waveguide. Parameters are given on Fig. 3. Tangential components of the electric and the magnetic fields are then continuous at the boundary, despite the phase jump. Incident and transmitted/coupled fields are obtained in the equation [Eq.1] :

$$\begin{bmatrix} E_{t1} \\ E_{t2} \end{bmatrix} = \begin{bmatrix} t & k \\ -k^* & t^* \end{bmatrix} \begin{bmatrix} E_{i1} \\ E_{i2} \end{bmatrix} \quad \text{Where} \quad |E_{t1}|^2 + |E_{t2}|^2 = |E_{i1}|^2 + |E_{i2}|^2$$

$$\text{and} \quad |t|^2 + |k|^2 = 1 \quad (1)$$

Following the above equation, it describe the relation between the incident fields (\mathbf{E}_{i1} and \mathbf{E}_{i2}) and the transmitted/coupled fields (\mathbf{E}_{t1} and \mathbf{E}_{t2}), the transmission with the coupling coefficients t and k , as well as the round-trip loss L . In the Matrix, we assume that the total input power equals the total output power and the summation of the coupler' transmission and coupling coefficients are equal to one. The propagation around the ring waveguide is in function of the loss coefficient L and the accumulated phase ϕ is described in

$$t = |t|e^{-j\phi_t}$$

equation [Eq.2]:

$$E_{i2} = E_{t2} \cdot L \cdot e^{-j\phi} \rightarrow E_{t1} = \frac{|t| - L \cdot e^{-j(\phi - \phi_t)}}{1 - |t|L \cdot e^{-j(\phi - \phi_t)}} E_{i1} e^{-j\phi_t} \quad (2)$$

Where $|t|$ refers to the transmission loss and the ϕ_t refers to the corresponding phase. The difference between the two phase (ϕ_t and ϕ) is integer value and promotional to 2π at the resonance frequency. At the critical coupling when $|t| = L$, transmission field is supposed to be equal to zero. Objective function is the improvement of the quality factor Q that is evaluated in term of λ_0 central resonance wavelength, $Q = \lambda_0 / \Delta\lambda$. The ranges of the parameters variation are chosen so as the coupling between the resonator and the optical fiber are always active. Finite element results at the resonance is described below.

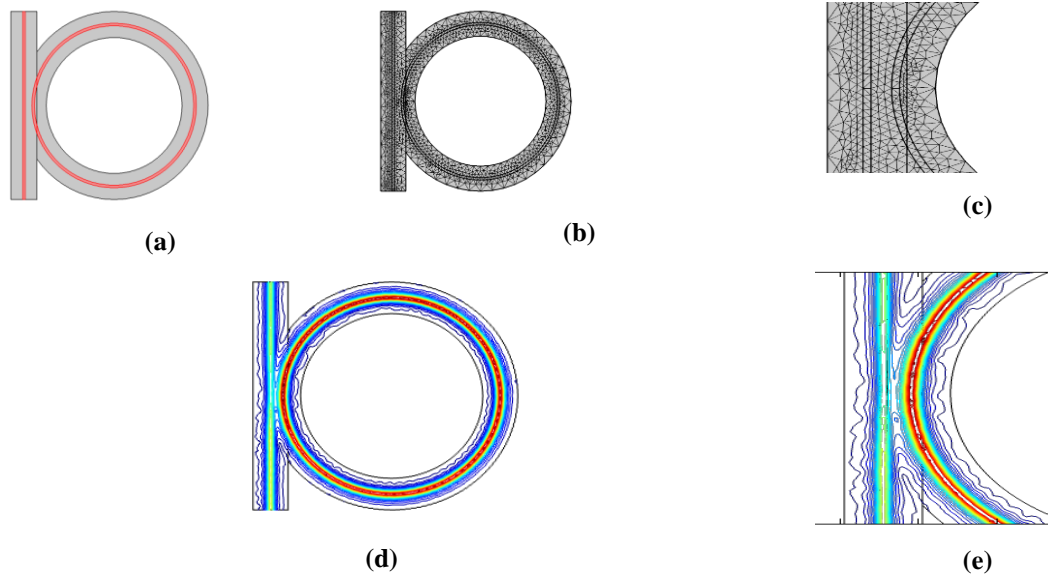


Fig. 4: Modeling and meshing of the waveguide (a, b & c) with *Finite element simulation of the coupled resonator based on the following assumption of optical symmetry and the Gallery mode in the resonator (d & e).*

The optimal quality factor Q obtained is quite similar to the one obtained by experimental. This should consolidate our finite element simulation and the coupled strategy for further optimizations. Fig. 4 indicates a result of simulation. The field continuity boundary condition between the straight waveguide and the ring waveguide allowed us to ensure that the tangential components of the electric and the magnetic fields are continuous at the boundary, despite the phase jump.

4. CONCLUSION

At this first step of the multi-physic optimization, we have demonstrated that we can simulate and find an optimal design. We can be extended this process to other application using coupled devices. Our sensitivity analysis shows a good correlation between Q -factor obtained with experiment and with finite element simulation. This optimization process may integrate later some constraints related to the manufacturing process, thermal analysis of the resonator so we can represent better at actual stage it can bring a great support to define better performances in several applications of these resonators in achieving high performances devices. Optimization of the model should bring a help to define better performances in several other applications of these resonators in achieving high performances devices [25 – 28] or sensors.

REFERENCES

- [1] Salzenstein P., Voloshinov V. B. and Trushin A. S., "Investigation in acousto-optic laser stabilization for crystal resonator based optoelectronic oscillators," *Optical Engineering* **52**(2), 024603 (2013).
- [2] Henriot, R., Salzenstein, P., Ristic, D., Coillet, A., Mortier, M., Rasoloniaina, A., Saleh, K., Cibiel, G., Dumeige, Y., Ferrari, M., Chembo, Y. K., Llopis, O., Féron, P., "High quality factor optical resonators," *Physica Scripta* **T162**, 014032 (2014).
- [3] Volyanskiy K., Salzenstein P., Tavernier H., Pogurmirskiy M., Chembo Y. K. and Larger L., "Compact Optoelectronic Microwave Oscillators using Ultra-High Q Whispering Gallery Mode Disk-Resonators and Phase Modulation," *Optics Express* 18(21), 22358-22363 (2010).

- [4] Henriet R., Coillet A., Salzenstein P., Saleh K., Larger L., Chembo Y.K., "Experimental characterization of optoelectronic oscillators based on optical mini-resonators," 2013 Joint EFTF and IFCS, 2013, pp. 37-39 (2013). DOI:10.1109/EFTF-IFC.2013.6702286.
- [5] Salzenstein P., "Frequency and temperature control for complex system engineering in optoelectronics and electronics: an overview," *Int. J. for Sim. and Mult. Design Optimization* 11, 7 (2020).
- [6] Braginsky V. B., Gorodetsky M. L., Ilchenko V. S., "Quality-factor and nonlinear properties of optical whispering-gallery modes," *Physics Letters A* **137**, 393-397 (1989).
- [7] Salzenstein P., Mortier M., Sérrier-Brault H., Henriet R., Coillet A., Chembo Y. K., Rasoloniaina A., Dumeige Y., Féron P., "Coupling of high quality factor optical resonators," *Physica Scripta* **T157**, 014024 (2013).
- [8] Salzenstein P., Diallo S., Zarubin M., "Electrically driven thermal annealing set-up dedicated to high quality factor optical resonator fabrication," *Journal of Power Technologies* **98**(2), 198-201 (2018).
- [9] Aissani M., Guessasma S., Zitouni A., *et al*, "Three-dimensional simulation of 304L steel TIG welding process: Contribution of the thermal flux," *Applied Thermal Engineering* **89**, 822-832 (2015).
- [10] Irisarri F. X., Bassir D. H., Maire J. F., Carrere N., "Multiobjective stacking sequence optimisation strategy for laminated composite structures," *Composites Science and Technology* **69**, 983-990 (2009).
- [11] Guessasma S., Bassir D., Hedjazi L., "Influence of interphase properties on the effective behaviour of a starch-hemp composite," *Materials and Design* **65**, 1053-1063 (2015).
- [12] Salzenstein P., Coillet A., Henriet H., Larger L., Yanne K. Chembo Y. K., " Experimental study of a crystalline-resonator based optoelectronic oscillator", *Proc. SPIE* **8772**, 87720O, (2013).
- [13] Luke K., Dutt A., Poitras C. B., Lipson M., "Overcoming Si₃N₄ stress limitations for high quality factor ring resonators," *Optics Express* **21**(19), 22829-22833 (2013).
- [14] Huang S.-W., Yang J., Lim J., Zhou H., Yu M., Kwong D.-L., Wong C. W., "A low-phase-noise 18GHz Kerr frequency microcomb phase-locked over 65THz," *Scientific Reports* **5**, 13355 (2015).
- [15] Gondarenko A., Levy J. S., Lipson M., "High confinement micron-scale silicon nitride high Q ring resonator," *Optics Express* **17**(14), 11366-11370 (2009).
- [16] Chen Y., Feng J., Zhou Z., Yu J., Summers C. J., Citrin D. S., "Fabrication of silicon microring resonator with smooth sidewalls," *J. Micro Nanolith MEMS MOEMS* **8**(4), 043060 (2009).
- [17] Marchal R., Labex Action, Post-doctoral report, Besançon, 29th August 2016, pp 8-9 (2016).
- [18] Bassir, D., Salzenstein P., "Optimal design of a crystalline and integrated resonator coupled with optical fibre" *Proc. SPIE* **10814**, 108140L (2018).
- [19] Salzenstein P., Dupuis O., Helal M., Lheurette E., Vanbésien O., Mounaix P., Lippens D., "Coplanar waveguides on dielectric membranes micromachined on GaAs substrate," *Electronics Letters* **32**(9), 821-822 (1996).
- [20] Bassir D., Salzenstein P., "Optimization of fiber to resonator coupling," *Proc. SPIE* **11357**, 113571P (2020).
- [21] Bassir D., Salzenstein P., Zhang M., "Optimization of coupled device based on optical fiber with crystalline and integrated resonators", *Proc. SPIE* **10228**, 102280Z (2017).
- [22] Hosseini E. S., Yegnanarayanan S., *et al*, "High Quality Planar Silicon Nitride Microdisk Resonators for Integrated Photonics in the Visible Wave length Range," *Optics Express* **17**, 14543-14551 (2009).
- [23] Guessasma S., Bassir D., "Optimization of the mechanical properties of virtual porous solids using a hybrid approach," *Acta Materialia* **58**(2), 716-725 (2010).
- [24] Bassir D. H., Guessasma S., "A Hybrid Computational Strategy for Identification of a Non Linear Composite Model," *Proc. of the Eighth International Conference on the Application of Artificial Intelligence to Civil, Structural and Environmental Engineering*, 2005. DOI:10.4203/ccp.82.37
- [25] Salzenstein P., Bassir D., Zarubin M., "Optimized oven for optical resonator heating process," *Proc. SPIE* **11334**, 1133406 (2019).
- [26] Salzenstein P., Pavlyuchenko E., Hmima A., Cholley N., Zarubin M., Galliou S., Chembo Y. K., Larger L., "Estimation of the uncertainty for a phase noise optoelectronic metrology system," *Physica Scripta* **T149**, 014025 (2012).
- [27] Salzenstein P., Wu T. Y., "Uncertainty analysis for a phase-detector based phase noise measurement system," *Measurement* **85**, 118-123 (2016).
- [28] Salzenstein P., Pavlyuchenko E., "Uncertainty Evaluation on a 10.52 GHz (5 dBm) Optoelectronic Oscillator Phase Noise Performance," *Micromachines* **12**(5), 474 (2021).